Characterization of Two Independent Amino Acid Substitutions that Disrupt the DNA Repair Functions of the Yeast Apn1†

Arshad Jilani,‡ Ratsavarinh Vongsamphanh,‡ Anick Leduc,‡ Laurent Gros,§ Murat Saparbaev,§ and Dindial Ramotar*,‡

Guy-Bernier Research Centre, University of Montreal, 5415 de l'Assomption, Montreal, Quebec, Canada H1T 2M4, and Groupe Reparation de l'ADN, Unite Mixte de Recherche 8532 CNRS, Laboratoire de Biotechnologies et Pharmacologie Genetique Appliquee-Ecole Normale Superieure Cachan, Institut Gustave Roussy, 94805 Villejuif Cedex, France

Received January 29, 2003; Revised Manuscript Received April 1, 2003

ABSTRACT: The members of the Endo IV family of DNA repair enzymes, including *Saccharomyces cerevisiae* Apn1 and *Escherichia coli* endonuclease IV, possess the capacity to cleave abasic sites and to remove 3′-blocking groups at single-strand breaks via apurinic/apyrimidinic (AP) endonuclease and 3′-diesterase activities, respectively. In addition, Endo IV family members are able to recognize and incise oxidative base damages on the 5′-side of such lesions. We previously identified eight amino acid substitutions that prevent *E. coli* endonuclease IV from repairing damaged DNA *in vivo*. Two of these substitutions were glycine replacements of Glu145 and Asp179. Both Glu145 and Asp179 are among nine amino acid residues within the active site pocket of endonuclease IV that coordinate the position of a trinuclear Zn cluster required for efficient phosphodiester bond cleavage. We now report the first structure−function analysis of the eukaryotic counterpart of endonuclease IV, yeast Apn1. We show that glycine substitutions at the corresponding conserved amino acid residues of yeast Apn1, i.e., Glu158 and Asp192, abolish the biological function of this enzyme. However, these Apn1 variants do not exhibit the same characteristics as the corresponding *E. coli* mutants. Indeed, the Apn1 Glu158Gly mutant, but not the *E. coli* endonuclease IV Glu145Gly mutant, is able to bind DNA. Moreover, Apn1 Asp192Gly completely lacks enzymatic activity, while the activity of the *E. coli* counterpart Asp179Gly is reduced by ∼40-fold. The data suggest that although yeast Apn1 and *E. coli* endonuclease IV exhibit a high degree of structural and functional similarity, differences exist within the active site pockets of these two enzymes.

Apurinic/apyrimidinic (AP)[1] sites, produced in cellular DNA both spontaneously and by many chemical mutagens (e.g., oxidative and alkylating agents), are highly genotoxic and must be repaired by AP endonucleases to prevent genetic mutations (*1*, *2*). The yeast *Saccharomyces cerevisiae* possesses a 40.5 kDa DNA repair enzyme, Apn1, which is localized to the nucleus as well as to the mitochondria (*3*−*5*). Apn1 is a key component of the base excision repair pathway, and functions to hydrolyze AP sites by cleaving the DNA backbone 5′ to the AP site to produce a 3′-hydroxyl group and a 5′-deoxyribose phosphate (*2*, *4*, *6*). The 5′-deoxyribose phosphate is then removed by a 5′-deoxyribose phosphodiesterase, such as yeast Rad27, to create a gap which is then filled and sealed by the sequential action of DNA polymerases and DNA ligase (*7*, *8*). Apn1 also possesses a 3′-diesterase activity, which removes a multitude of 3′-blocking groups (e.g., 3′-phosphoglycolate and 3′-phosphate) at DNA single-strand breaks induced by oxidative agents, including the antitumor drug bleomycin and hydrogen peroxide (H_2O_2) (*6*, *9*). More recently, we have shown that Apn1 recognizes and cleaves oxidized bases immediately 5′ to the lesion to create a 3′-hydroxyl group (*10*). This enzyme is also able to act on nicked DNA to remove the 3′-nucleotide, thereby generating a single-nucleotide gap (*10*). Thus, Apn1 can be viewed as having multiple enzymatic activities.

Mutants lacking Apn1 (*apn1*Δ) are hypersensitive to the alkylating agent methyl methane sulfonate (MMS) due to defective repair of MMS-induced AP sites (*4*), and also display a 10−15-fold increase in the rate of spontaneous AP site-induced single-base pair mutations (*11*−*13*). *apn1*Δ mutants are not sensitive to agents that generate DNA strand breaks with blocked 3′-termini due to the presence of another compensating AP endonuclease/3′-diesterase activity, i.e., Apn2 (also called Pde1 and Eth1) (*14*, *15*). When both *APN1* and *APN2* genes are deleted, the resulting *apn1*Δ*apn2*Δ

† This work was partially funded by the National Cancer Institute of Canada (NCIC) with funds from the Canadian Cancer Society and the Natural Sciences and Engineering Research Council of Canada (D.R.) and by European Community Grant QLK4-2000-00286 and Association pour la Recherche sur le Cancer (M.S.). D.R. is supported by a senior fellowship from the Fonds de la Recherche en Sante du Quebec, and L.G. is supported by a postdoctoral fellowship from European Community.

* To whom correspondence should be addressed. E-mail: dramotar@hmr.qc.ca. Telephone: (514) 252-3400, ext 4684. Fax: (514) 252-3430.

‡ University of Montreal.

§ Institut Gustave Roussy.

[1] Abbreviations: AP, apurinic/apyrimidinic; endo IV, endonuclease IV; MMS, methyl methane sulfonate; H_2O_2, hydrogen peroxide; IPTG, isopropyl thio-β-D-galactoside; DTT, dithiothreitol; UDG, uracil DNA glycosylase; DHU, 5,6-dihydrouracil; DHT, 5,6-dihydrothymine; THF, tetrahydrofuran.

10.1021/bi034163m CCC: $25.00
Published on Web 05/08/2003

double mutant is exquisitely sensitive to MMS, and displays hypersensitivity to agents such as H_2O_2 that create strand breaks terminated with 3′-blocking groups (*15*).

Apn1 belongs to the Endo IV family of DNA repair enzymes, which is exemplified by *Escherichia coli* endonuclease IV (endo IV) (*2*). Recent studies have shown that Apn1/endo IV homologues also exist in the fission yeast *Schizosaccharomyces pombe*, as well as in the nematode *Caenorhabditis elegans*, underscoring the importance of Endo IV family members in the repair of damaged DNA (*2*). These members share five highly conserved regions (RI−RV) that are distributed along the entire length of the proteins (*2*). For example, the RIII region contains a stretch of amino acid residues (KSRxGVCIDTCHxFAxGYD) that are identical in all members (*2*). Consistent with this substantial degree of amino acid sequence homology, cross-species complementation revealed that Endo IV family members are also highly functionally conserved. For example, yeast Apn1 can substitute for *E. coli* endo IV and *vice versa* (*16*). However, despite the high degree of evolutionary conservation among Endo IV family members, no corresponding homologue has yet been found in human cells (*2*).

We have been interested in elucidating the mechanism by which *E. coli* endo IV recognizes and cleaves phosphodiester bonds at sites of DNA damage. Using chemical mutagenesis, we previously identified eight essential amino acid substitutions that alter endo IV function with respect to both AP site cleavage and removal of blocked 3′-termini (*17*). Indeed, mutants bearing these substitutions showed parallel reductions of AP endonuclease/3′-diesterase activities, ranging from 10- to 150-fold (*17*). One of the mutants, bearing the E145G substitution located in the conserved region RII, actually prevented endo IV from binding to DNA (*17*). Other substitutions destabilized the protein and were deemed essential for the proper maintenance of the tertiary structure (*17*). Concurrent with our reported findings, the high-resolution atomic structure of endo IV was published and assigned the side chain of nine amino acid residues as coordinating a trinuclear Zn cluster within the active site pocket of the enzyme. Among our own panel of endo IV mutants are variants in which two of these nine amino acid residues (i.e., either Glu145 or Asp179) have been replaced with glycine (*17*). We therefore set out to investigate if the corresponding conserved amino acid residues of Apn1 (i.e., Glu158 and Asp192) are also essential for biological function. Our data clearly reveal that glycine substitution at either Glu158 or Asp192 of Apn1 prevents the mutant protein from repairing damaged DNA *in vivo*, although these mutants differ substantially from their endo IV mutant counterparts. We suggest that Apn1 and endo IV use slightly different mechanisms to catalyze the processing of damaged DNA.

MATERIALS AND METHODS

Strains, Media, Genetic Analysis, and Transformation. The bacterial strains used in this study were the parent AB1157 and the mutant BW528 [Δ(xth-pnc), nfo1::kan)] (kindly provided by B. Weiss, Emory University, Atlanta, GA). The bacteria were transformed with the indicated vector or plasmid (see below) by the $CaCl_2$ method. The *E. coli* strain used for plasmid maintenance was DH5α. The *S. cerevisiae* strains used in this work were YW465 (MATα;ade2Δ0 his3Δ-200 leu2Δ-1 met15Δ0 trp1Δ-63 ura3Δ0), YW605 (isogenic to YW465, except *apn1*Δ*::HIS3*), and YW781 (isogenic to YW465, except *apn1*Δ*::HIS3 apn2*Δ*::KanMX4*) and were generously provided by T. Wilson (Ann Arbor, MI). Yeast cells were grown in either complete yeast peptone dextrose (YPD) or minimal synthetic (SD) medium, to which standard nutritional supplements had been added at 20 μg/mL. Transformation were carried out as described previously (*18*).

Construction of the Plasmids GFP-APN1 and GST-APN1. The full-length *APN1* gene (bp −13 to 1383) was amplified by polymerase chain reaction (PCR) from the plasmid YepApn1 using the primers APN1-F1-*Eco*RI (5′-$^{-13}$CGGAACCATCGAATTCCCTTCGACACCTAGCTTTG^{21}-3′) and DR-2B (5′-^{1383}CCATAAGAGGATGGTCGACCGCCTTCCTTAG^{1353}-3′) bearing the restriction sites (underlined) for *Eco*RI and *Sal*I, respectively. The amplified 1.4 kb DNA fragment was digested with *Eco*RI and *Sal*I and subcloned next to the green fluorescent protein (Gfp) gene, which is under the control of the *GAL1* promoter in the yeast expression vector pYES2.0, to produce the plasmid pGFP-APN1. In a similar fashion, the fragment was cloned next to the glutathione *S*-transferase (Gst) gene and placed under the control of the *lac* promoter in the *E. coli* expression vector pGEX-4T-1 (Amersham Pharmacia Biotech) to produce the plasmid pGST-APN1.

Site-Directed Mutagenesis. Single-amino acid mutations within the *Apn1* protein were created by the QuickChange site-directed mutagenesis kit (Stratagene) using the pGST-APN1 plasmid as the template. The two oligonucleotides used for creating the E158G mutation were ApnE158up (5′-GTTAAAATTGTATTAG**G**AAATATGGCTGGTACTGG-3′) and ApnE158Gdwn (5′-CCAGTACCAGCCATATTT-**C**CTAATACAATTTTAAC-3′) bearing the centrally located changes in bold, that is, switching GAA to G**G**A. The two oligonucleotides used for creating the D192G mutation were ApnD192Gup (5′-GAATCGGCGTTTGCATAG**G**TACATGCCATACATTTG-3′) and ApnD192Gdwn (5′-CAAATGTATGGCATGTA**C**CTATGCAAACGCCGATTC-3′), bearing the centrally located changes in bold, that is, switching GAT to G**G**T. The mutations in the resulting plasmids pGST-APN1(E158G) and pGST-APN1(192G) were verified by DNA sequence analysis using the primer ApnSeqA (5′-GAAAGGAGACCATCAGTTGCAG-3′).

Construction of pGFP-APN1(E158G) and pGFP-APN1-(D192G). The plasmids pGST-APN1(E158G) and pGST-APN1(D192G) were digested with *Eco*RI and *Sal*I to release the DNA fragments encoding the indicated *APN1* allele and cloned next to the *GFP* as above to produce pGFP-APN1 E158G and pGFP-APN1 D192G.

Gradient Plate Assay. This assay was performed as previously described (*16*). Briefly, cells were replicated as a thin line along the drug gradient, and photographed after growth for 24 h at 37 °C. Growth along the gradient (∼82 mm) is considered to be 100%.

Immunodetection. The proteins were separated on a 10% SDS−PAGE gel and transferred onto a nitrocellulose membrane (8 cm × 10 cm) (Amersham Life Science) which was then blocked with TSE [10 mM Tris-HCl (pH 7.45), 150 mM NaCl, 0.1% Tween, and 1 mM EDTA] containing 5% powdered milk for 1 h. The membrane was probed for 16 h at 4 °C with 10 mL of TSE containing anti-Gfp

monoclonal antibodies at a dilution of 1:5000. Following the probing, the membrane was washed three times for 15 min each time with TSE before addition of 10 mL of the anti-mouse IgG conjugated to horseradish peroxidase at a dilution of 1:2500 (BIO/CAN Scientific, Inc.) for 1 h at room temperature. Finally, the membrane was washed again three times for 15 min each time with TSE, and immunoreactive polypeptides were detected by chemiluminescence (Dupont-NEN).

Purification of Apn1, Gst-Apn1, and the Mutant Forms. BW528 cells bearing the plasmids pGST-APN1, pGST-APN1(E158G), and pGST-APN1(D192G) were grown overnight at 30 °C in 8 mL of LB medium containing 100 μg/mL ampicillin, and then subcultured into 250 mL of LB medium containing 100 μg/mL ampicillin to an OD of 0.6 at 600 nm. IPTG (Sigma) was then added to a final concentration of 1 mM, and the culture was grown for an additional 140 min. Cell pellets were resuspended in 2.5 mL of buffer A which consisted of 50 mM Tris-HCl (pH 7.5), 100 mM NaCl, 0.5 mM EDTA, 0.5 mM DTT, and the protease inhibitor cocktail (Complete Mini, EDTA-free, Roche Diagnostics GmbH). Cell extracts were prepared as previously described (*19*) with the slight modification of using three freeze−thaw cycles (freezing in an ethanol/dry ice freezing bath and thawing at 37 °C). Extracts were then sonicated for 2 × 5 s (at 50% power) and centrifuged at 12 000 rpm at 4 °C, and the supernatants were loaded onto a 0.25 mL glutathione-Sepharose 4B mini column (Amersham Pharmacia Biotech) pre-equilibrated with buffer A. The column was washed three times with buffer A and eluted with 500 μL of 50 mM Tris-HCl (pH 8.0) containing 10 mM reduced glutathione. The eluted proteins were dialyzed in a Spectra/Por 1 dialysis tube (MWCO 6K-8K, Spectrum) against 500 mL of buffer A for 3 h with three intervening changes. The dialyzed proteins were loaded onto a 50 μL Macro-Prep 50S (Bio-Rad) mini column pre-equilibrated in buffer A, and the flow-through fractions containing the Gst-Apn1 or the Gst-Apn1 mutants were collected and concentrated in a 4.0 mL capacity 10K cutoff Ultrafree Biomax concentrator (Millipore Corp.) to 150 μL. The concentrations of the proteins were determined according to the method of Bradford (*20*).

The open reading frame DNA encoding Apn1 was cloned into pET11a (Novagen, Madison, WI) and the protein overexpressed in *E. coli* BL21 Star cells (Invitrogen SARL, Gergy Pontoise, France). Purification of the protein was achieved using three chromatographic steps: DEAE-sepharose (Waters), sulfopropyl Sepharose cation exchange (Amersham Biosciences, Little Chalfont, U.K.), and AcA54 gel filtration (IBF, Villeneuve-la-Garenne, France).

AP Endonuclease and 3′-Diesterase Assays. For the AP endonuclease assay, a 42-mer U21·G oligo (5′-GCTGCATGCCTGCAGGTCGA**U**TCTAGAGGATCCCGGGTACCT-3′) containing a single uracil at position 21 was labeled at the 5′-end by T4 polynucleotide kinase (PNK) (Gibco) using [γ-^{32}P]ATP (Pharmacia), and annealed to the complementary 42-mer oligo (3′-CGACGTACGGACGTCCAGCT**G**AGATCTCCTAGGGCCCATGGA-5′) to generate the U·G mismatch (*21*). To create the AP site substrate, this labeled double-stranded oligonucleotide was treated with uracil DNA glycosylase (UDG) for 30 min at 37 °C. The AP endonuclease assay and product resolution by urea−PAGE were performed as previously described (*17*). To generate the 3′-blocked termini, the labeled double-stranded oligonucleotide was treated with endonuclease III (kindly provided by Dr. Melamede, University of Vermont, Burlington, VT) at 37 °C for 1 h to convert all the AP sites into 3′-blocked ends. The 3′-diesterase assay and analysis of the reaction product by urea−PAGE were performed as previously described (*17*).

DNA Glycosylase-Independent Incision of Oxidatively Damaged DNA. Oligodeoxyribonucleotides were purchased from Eurogentec (Seraing, Belgium), including modified oligonucleotides containing either 5,6-dihydrouracil (DHU), 5,6-dihydrothymine (DHT), or tetrahydrofuran (THF) residues: 5′-TGACTGCATA**X**GCATGTAGACGATGTGCAT-3′ (30-mer), where X is the position of the modified base, DHU or DHT. The complementary oligonucleotides contained either dG or dA opposite the modified base. The resulting duplex oligonucleotides were termed dHU/G and dHT/A, respectively. This sequence context was previously used to study the repair of a thymine fragmentation product (*22*). Oligonucleotides were 5′-end labeled by T4 polynucleotide kinase (New England Biolabs, Beverly, MA) in the presence of [γ-^{32}P]ATP (6000 Ci/mmol, ICN Pharmaceuticals, Inc., Costa Mesa, CA) or 3′-end labeled by terminal transferase (New England Biolabs) in the presence of [α-^{32}P]dCTP (3000 Ci/mmol, Amersham Biosciences, Piscataway, NJ) as recommended by the manufacturers. The oligonucleotides were then annealed to the appropriate complements in buffer containing 0.5× SSC [75 mM NaCl and 7.5 mM citric acid trisodium salt (pH 7.0)] at 65 °C for 5 min as previously described (*23*). For determination of nucleotide incision activity, 0.4 pmol (or 0.2 pmol for THF/G oligonucleotide) of 5′-[^{32}P]- or 3′-[^{32}P]dCMP-labeled oligonucleotide duplex was incubated with 10 ng (or 5 ng for THF/G oligonucleotide) of the given repair protein(s) for 30 min (or 10 min for THF/G oligonucleotide) at 37 °C in reaction buffer (20 μL) containing 50 mM HEPES (pH 7.5), 50 mM KCl, 0.1 mM EDTA, 5 mM β-mercaptoethanol, and 0.1 mg/mL BSA. When necessary, a light piperidine treatment was performed by adding 10% piperidine for 15 min at 37 °C. Reaction products were analyzed by electrophoresis on denaturing 20% polyacrylamide gels (20:1, 7 M urea, 0.5× TBE) and visualized with a Storm 840 PhosphorImager (Molecular Dynamics Inc.).

Electrophoretic Mobility Shift Assay. A 5′-^{32}P-end-labeled 42-mer double-stranded oligonucleotide was used as a probe for the EMSA. Assays were performed as described previously (*17*). In brief, approximately 0.1 ng of the labeled probe (corresponding to 1.5 × 10^4 cpm) was incubated with 15 ng of wild-type and mutant Apn1 proteins in buffer B [10 mM Hepes-NaOH (pH 7.9), 20 mM KCl, 10% glycerol, 0.1 mM EDTA, 0.5 mM DTT, and 1 mM PMSF] for 20 min at room temperature. The formation of protein−DNA complexes was resolved by electrophoresis in a 140 cm × 175 cm × 0.75 cm, 6% native polyacrylamide gel (19:1 acrylamide:bisacrylamide ratio) in high-ionic strength Tris-glycine buffer [50 mM Tris-HCl (pH 8.8), 380 mM glycine, and 2 mM EDTA] at 100 V for 4 h at 4 °C, dried, and revealed by autoradiography (*24*). The sequences of the two different probes, 42-mer U·G and 42-mer C·G double-stranded oligonucleotides, were 5′-GCTGCATGCCTGCAGGTCGA**U**TCTAGAGGATCCCGGGTACCT-3′ and the complementary strand 3′-CGACGTACGGACGTCCAGCT**G**AGATCTCCTAGG-

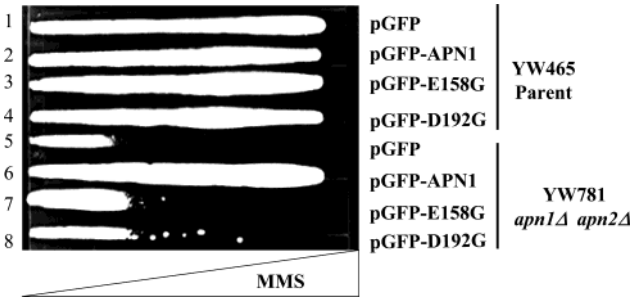

FIGURE 1: Drug resistance determination in *S. cerevisiae* strains YW465 (parent) and YW781 (*apn1*Δ*apn2*Δ) harboring plasmids carrying either the native or mutant alleles of the *APN1* gene fused to GFP. The results were obtained from gradient plate assays where the bottom layer contained 0.015 mmol of methyl methane sulfonate (MMS). Growth along the gradient is considered to be 100%. The picture was taken after incubation for 1 day at 30 °C.

GCCCATGGA-5′ and 5′-GGTCTAAACGTTTATGCCTTT-GCTCTGGACCATACAATTATC-3′ and the complementary strand 3′-CCAGATTTGCAAATACGGAAACGAGA-CCTGGTATGTTAATAG-5′, respectively.

RESULTS

The Construct GFP-APN1 Expresses a Functionally Active Fusion Protein. The full-length *APN1* gene was inserted in frame into the pYES-GFP vector to produce the plasmid pGFP-APN1, which expresses the Gfp-Apn1 fusion protein under the galactose inducible *GAL1* promoter (see below and Materials and Methods) (*5*). To examine if the plasmid expressed a functionally active Gfp-Apn1 fusion protein, we tested for drug complementation in strain YW781-(*apn1*Δ*apn2*Δ) (*25*). This strain lacks both Apn1 and Apn2, and therefore is hypersensitive to various DNA-damaging agents, including MMS and H_2O_2, which that produce AP sites and strand breaks with blocked 3′-termini, respectively (*15*, *25*). Introduction of pGFP-APN1 into strain YW781 conferred full parental resistance to MMS (Figure 1, lane 6) and H_2O_2 (data not shown), under noninducing conditions, as determined by gradient plate assays. In this assay, the drug-sensitive strains grow only a short distance into the gradient, whereas the resistant strains grow along the entire length of the gradient (*16*). As expected, the pYES-GFP vector provided no drug resistance to strain YW781 (Figure 1, lane 5). The data suggest that plasmid pGFP-APN1 produces a biologically active fusion protein in yeast cells. It is noteworthy that the *GAL1* promoter is leaky and produces enough Gfp-Apn1 to restore drug resistance to strain YW781. Overproduction of Gfp-Apn1 by galactose induction conferred no additional drug resistance to strain YW781 (data not shown). Similar findings were previously observed in yeast with untagged Apn1 (*3*, *4*).

The Gfp-Apn1(E158G) and Gfp-Apn1(D192G) Mutant Plasmids Confer No Drug Resistance to the AP Endonuclease Deficient Strain YW781. We determined if glycine substitution of amino acid residues E158 and D192 interferes with the biological function of Apn1. The two substitutions, E158G and D192G, were created by altering the DNA sequence in plasmid pGFP-APN1 by site-directed mutagenesis to produce the plasmids pGFP-APN1(E158G) and pGFP-APN1(D192G), respectively. Introduction of either mutant plasmid into strain YW781 failed to confer resistance to MMS or H_2O_2, as compared to the native pGFP-APN1 plasmid (Figure 1, lanes 7 and 8 vs lane 6, and data not shown). Similar results were obtained if the drug gradient plate assays were carried out under conditions of galactose induction (data not shown). The data suggest that the plasmids pGFP-APN1(E158G) and pGFP-APN1(D192G) are likely expressing inactive mutant proteins.

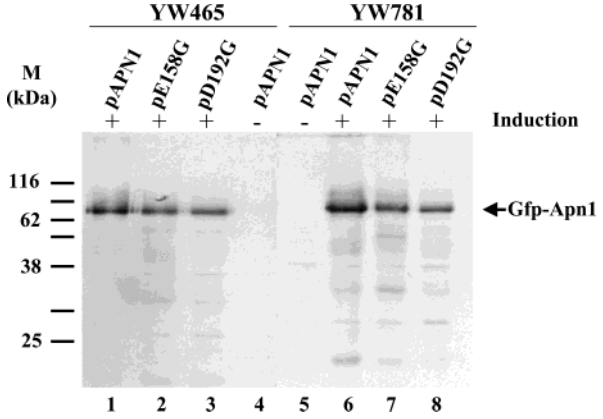

FIGURE 2: Comparison of the expression levels of native Apn1 and its mutant forms fused to Gfp. Total protein extracts were derived from the indicated plasmid-bearing yeast strains YW465 and YW781 following induction for 4 h with (+, lanes 1−3 and 6−8) or without (−, lanes 4 and 5) 0.5% galactose. Each lane contains 100 μg of total extract, and the Western blot was probed with a monoclonal anti-Gfp antibody. The arrow indicates the position of the native and mutant forms of Gfp-Apn1 (66 kDa). Molecular mass standards are shown at the left.

The Apn1 Mutant Plasmids Express Normal Levels of the Mutant Proteins and Are Localized to the Nucleus. To exclude the possibility that the lack of complementation by these mutant plasmids might merely reflect a reduction in the level of protein expression, we examined levels of native and mutant proteins in total cell extracts (Figure 2). Extracts derived from either the parent, or strain YW781 harboring the native plasmid pGFP-APN1, expressed the expected 66 kDa full-length fusion protein following galactose induction (0.5% for 4 h) (Figure 2, lanes 1 and 6, respectively). In the absence of galactose induction, the Gfp-Apn1 fusion protein could not be detected with anti-Gfp antibodies (lanes 4 and 5), although under these conditions enough Gfp-Apn1 is expressed to fully restore drug resistance to strain YW781 (Figure 1). Total extracts prepared from either the parent or strain YW781 harboring either of the two mutant plasmids also exhibited normal expression levels of the 66 kDa fusion protein (Figure 2, lanes 2, 3, 7, and 8, respectively). There was no significant degradation of either mutant fusion protein, suggesting that these do not exhibit any major structural deformation to trigger proteolysis, and thus are as stable as the native fusion protein. Another possibility that could explain the inability of the Apn1 mutants to complement the drug hypersensitive phenotypes of strain YW781 might involve prevention of protein translocation into the nucleus. We therefore examined the cellular location of the native and mutant proteins by immunofluorescent microscopy (see Materials and Methods). The native Gfp-Apn1 and the Apn1 mutants were mainly localized to the nucleus in both strains following induction with galactose (Figure 3). We conclude that the two plasmids pGFP-APN1(E158G) and pGFP-APN1(D192G) are indeed expressing normal levels of mutant protein, and that the mutant proteins do not harbor a defect in entering the nucleus, supporting the notion that

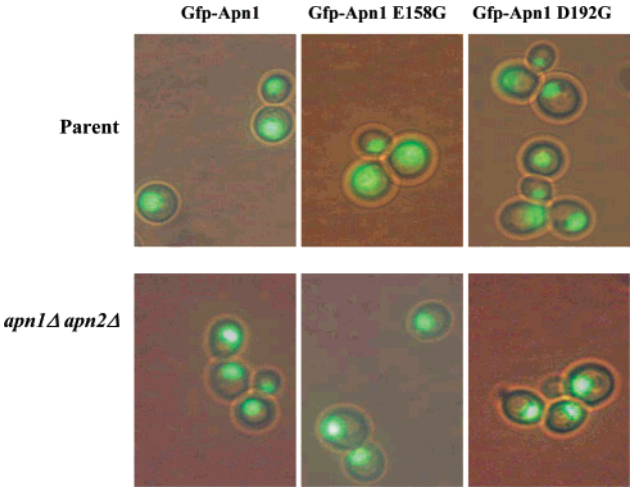

FIGURE 3: Nuclear localization of Gfp-Apn1 and its mutant forms. Immunofluorescent analysis was performed with strains YW465 (parent) and YW781 (*apn1*Δ*apn2*Δ) (YW778) bearing either the pGFP-APN1, pGFP-APN1(E158G), or pGFP-APN1(D192G) plasmid. Cells were grown in selective medium with 2% raffinose and induced with 0.5% galactose for 4 h before being photographed at a magnification of 100 times with a Cool Snap camera attached to a Leitz immunofluorescent microscope.

these mutant proteins lack the ability to repair damaged DNA.

Expression and Complementation Analyses of Gst-Apn1 and the Gst-Apn1 Mutant Forms in the DNA Repair Deficient E. coli Strain BW528. To determine if the Apn1(E158G) and Apn1(D192G) mutants have a defect in repairing damaged DNA, we designed an *E. coli* expression system to facilitate the purification of these proteins. The genes encoding the native *APN1* and the two mutant alleles, *APN1*(*E158G*) and *APN1*(*D192G*), were inserted in frame next to the glutathione *S*-transferase gene *Gst* in the vector pGEX-4T-1 to create a set of three plasmids [pGST-APN1, pGST-APN1(E158G), and pGST-APN1(D192G)], which were designed to produce Gst-Apn1, Gst-Apn1(E158G), and Gst-Apn1(D192G) fusion proteins, respectively, under the control of the IPTG-inducible *lac* promoter. The plasmids were introduced into *E. coli* strain BW528, which in a manner analogous to that of its yeast counterpart strain YW781 is deficient in AP endonuclease activity, i.e., is lacking both endonuclease IV and exonuclease III genes. This *E. coli* strain is also hypersensitive to various DNA-damaging agents because of an inability to repair damaged chromosomal DNA (*26*). Total extracts derived from the exponentially growing *E. coli* strain BW528 carrying either plasmid pGST-APN1, pGST-APN1(E158G), or pGST-APN1(D192G), and induced by IPTG, expressed the expected 66 kDa fusion protein as observed by Coomassie staining (Figure 4A). The expression levels were similar for all three proteins, and no major degradation was observed (Figure 4A).

We previously showed that expression of Apn1 complemented the drug hypersensitivities of strain BW528 (*26*). We therefore tested if the fusion form of Apn1, Gst-Apn1, was also capable of complementing the drug hypersensitivites of strain BW528. Introduction of the plasmid pGST-APN1 into strain BW528, but not the empty pGST vector (pGEX-4T-1), restored parental resistance to both MMS and H_2O_2 (Figure 5A,B, lane 3 vs lane 5), suggesting that the Gst-Apn1 fusion protein is functionally active in bacteria, as is the Gfp-Apn1 fusion protein in yeast. It should be noted that the *lac* promoter appears to be leaky since the drug complementation assay was performed in the absence of IPTG (Figure 5). However, in the presence of IPTG, Gst-Apn1 conferred no additional drug resistance to strain BW528 (data not shown). This is not surprising, as we have documented similar findings with the overexpression of Apn1 in strain BW528 (*26*). Introduction of the mutant plasmids, either pGST-APN1(E158G) or pGST-APN1(D192G), into BW528 conferred no resistance to MMS or H_2O_2 (Figure 5A,B, lanes 1 and 2), clearly indicating that the mutant proteins expressed by these plasmids are unable to act on the damaged DNA.

Apn1 Mutants Lack DNA Repair Activities. We next examined the ability of the purified Gst-Apn1 fusion protein and the mutant forms to process DNA lesions *in vitro*. Briefly, the Gst fusion proteins were affinity-purified on a glutathione column followed by ion-exchange chromatography on monoS (panels B and C of Figure 4, respectively). This second purification step was necessary to remove trace contamination of AP lyase activity, which bound to the Gst affinity column independent of Apn1. The purified Gst fusion proteins were assessed for all three enzymatic activities, i.e., AP endonuclease, 3′-diesterase, and the activity that incises oxidized base lesions. To monitor AP endonuclease activity, we used a labeled 42-mer double-stranded oligonucleotide bearing a single AP site at position 21. Cleavage of the AP site substrate by AP endonucleases produces a labeled 20-mer product which can be readily detected on 10% polyacrylamide gels (*21*). As shown in Figure 6A, the native Gst-Apn1, as well as purified endo IV, actively cleaved the substrate to produce the 20-mer product (lanes 1, 2, and 7). Interestingly, following the formation of the 20-mer product, purified Gst-Apn1 was able to remove additional nucleotides in a 3′- to 5′-direction to create a smaller product (lane 1 or 2), but not the mutants even at higher protein concentrations (>50 ng, data not shown). We further note that the 3′- to 5′-exonuclease activity is unlikely to be the result of a bacterial contaminant that is copurified with Gst-Apn1, as this activity was not detected with the mutant when incubated with the endo IV pre-incised AP site (data not shown). These data suggest that Apn1 may possess a 3′- to 5′-exonuclease activity (see the Discussion).

Analysis of the Gst-Apn1(E158G) mutant revealed that it was highly inefficient at cleaving the AP site substrate (Figure 6A, lane 4 vs lane 2). In separate experiments, we estimated that the Gst-Apn1(E158G) mutant exhibited a nearly 150-fold reduction in AP endonuclease activity, compared to that of the native Gst-Apn1 (data not shown). In contrast, the Gst-Apn1(D192G) mutant exhibited no detectable cleavage activity even at protein concentrations in excess of 200-fold (Figure 6A, lane 6 vs lane 2, and data not shown). These findings clearly indicate that the glycine amino acid substitution at either position 158 or 192 dramatically reduces or completely abolishes the AP endonuclease activity of Apn1, respectively, such that the resulting mutant proteins cannot repair MMS-induced AP sites in the DNA repair deficient strains.

We next monitored the 3′-diesterase activity of these proteins by following the removal of a 3′-blocking DNA lesion, 3′-α,β-unsaturated aldehyde. To create this lesion, the 42-mer oligonucleotide substrate containing the AP site

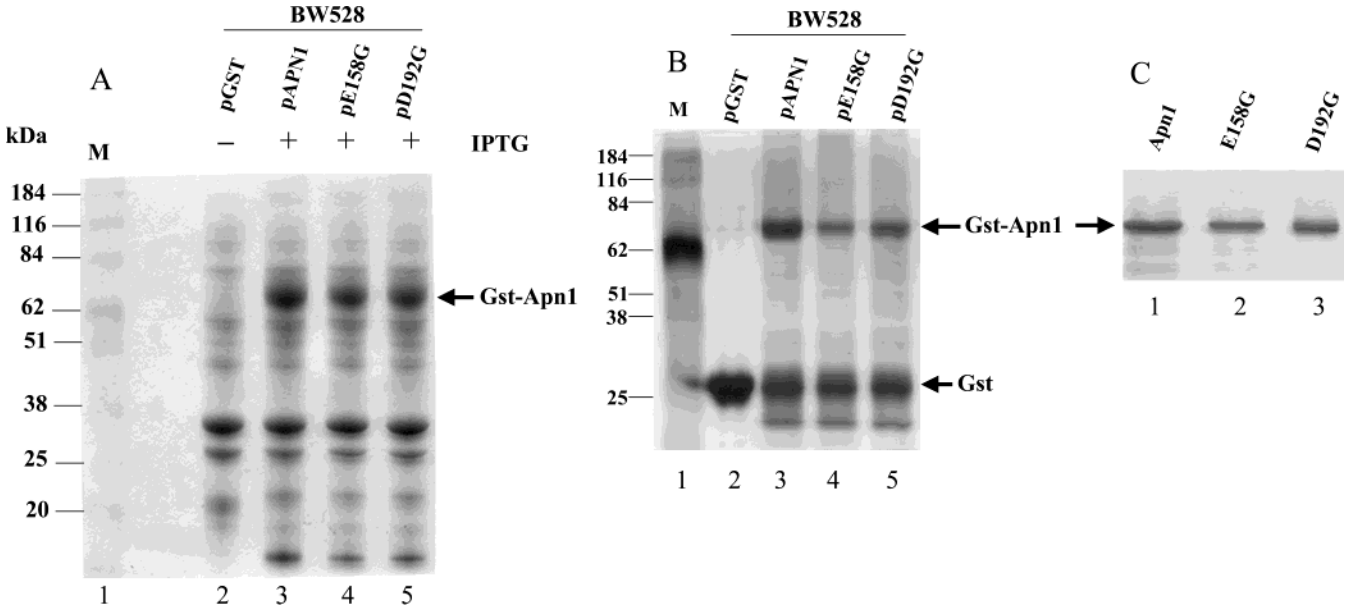

FIGURE 4: Expression and purification of native and mutant forms, E158G and D192G, of Apn1 using *E. coli*. (A) Coomassie blue-stained SDS−PAGE gel of total extracts derived from strain BW528, and carrying either the pGST vector, the pGST-APN1 plasmid, or the mutant forms: lane 1, molecular mass standards; and lanes 2−5, pGST, pGST-APN1(pAPN1), pGST-APN1(pE158G), and pGST-APN1(pD192G), respectively. Each lane (lanes 2−5) contained 60 μg of total protein extract. The plus and minus signs indicate whether the lane did or did not experience 1 mM IPTG induction. (B) Glutathione *S*-transferase affinity column purification of Gst-Apn1 and its mutant forms. Total extracts derived from strain BW528 carrying either the pGST, pGST-APN1(pAPN1), pGST-APN1(E158G), or pGST-APN1(D192G) plasmid were purified on a Gst affinity column and analyzed on an SDS−PAGE gel stained with Coomassie blue. Each lane (lanes 2−5) contained 200 ng of the affinity-purified proteins. (C) Gst affinity-purified Apn1 and the variants were subjected to ion-exchange chromatography on monoS and analyzed on a Coomassie-stained gel. Each lane (lanes 1−3) contained 200 ng of purified protein. For each panel, the arrow indicates the position of the native and mutant forms of the fusion protein, Gst-Apn1.

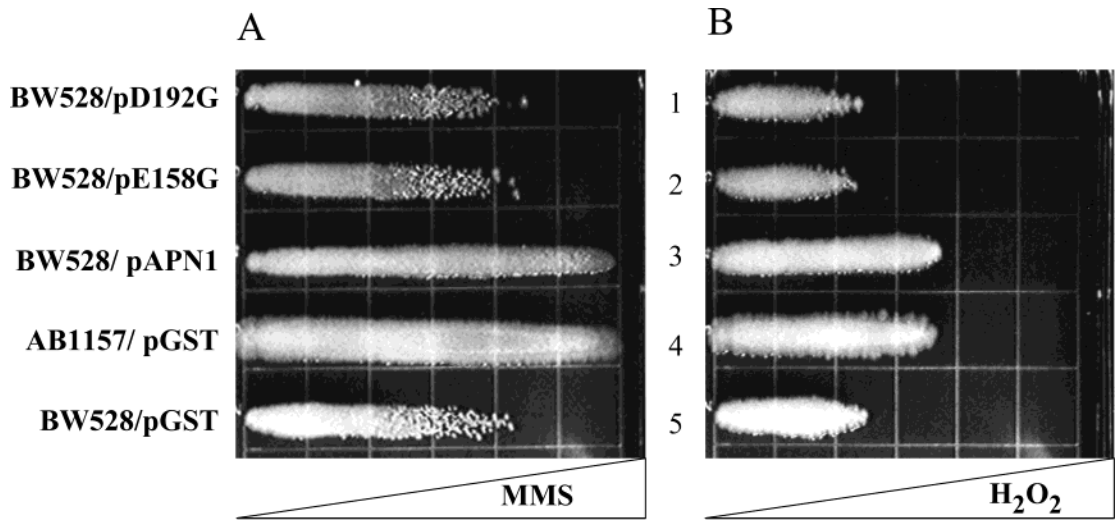

FIGURE 5: Drug complementation analysis of strain BW528 carrying plasmids expressing the native and mutant forms of Apn1 fused to Gst. AB1157(endoIV$^+$exoIII$^+$) is the parent of BW528(endoIV$^-$exoIII$^-$). The complementation assays were performed on drug gradient plates with the bacterial strains bearing plasmids with the indicated Gst-APN1 fusion genes. The bottom layer of the gradient plate contained either 0.025 mmol of MMS (A) or 1.17 mM H_2O_2 (B). Growth along the gradient is considered to be 100%. Pictures were taken after incubation for 24 h at 37 °C.

was pretreated with the AP lyase endonuclease III, which cleaves the AP site by a β-elimination reaction 3′ to the AP site, to generate the 20-mer product containing, at the 3′-end, *trans*-4-hydroxy-2-pentenal 5-phosphate (3′-α,β-unsaturated aldehyde) (Figure 6B). This endonuclease III preparation is contaminated with Fpg, an enzyme that can cleave AP sites to generate a 3′-phosphate (Figure 6B). Thus, the *trans*-4-hydroxy-2-pentenal 5-phosphate (3′-α,β-unsaturated aldehyde) product also contained a minor amount of 3′-phosphate (Figure 6B). Both the 3′-α,β-unsaturated aldehyde and the 3′-phosphate can be removed by a 3′-diesterase activity to create the intermediate migrating 20-mer containing a 3′-hydroxyl group (Figure 6B). As shown in Figure 6B, the native Gst-Apn1 actively processed the 3′-α,β-unsaturated aldehyde and the 3′-phosphate to generate the 20-mer product bearing the 3′-hydroxyl group, which migrated to the same position as the product produced by direct AP endonuclease action, such as endonuclease IV on the 42-mer AP site substrate. In contrast, neither of the Gst-Apn1 mutants was capable of removing the 3′-blocking groups (Figure 6B, lane 3 or 4, and lane 5 or 6). Thus, substitution of amino acid residues E158 and D192 of Apn1

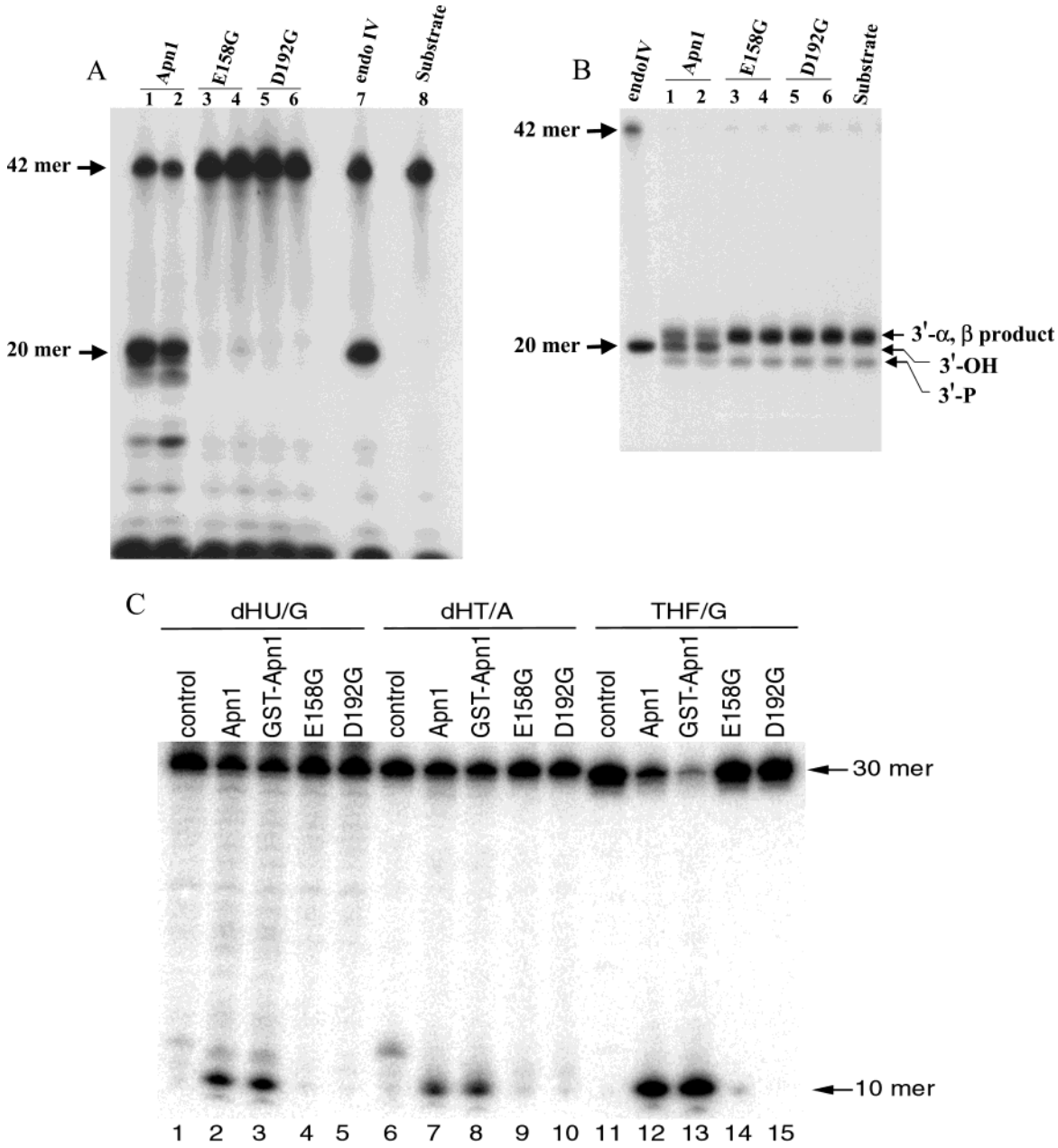

FIGURE 6: Comparison of the DNA repair activities of Apn1 and the mutant forms, E158G and D192G. (A) Analysis of the AP endonuclease activity. The 5′-^{32}P-labeled 42-mer double-stranded oligonucleotide U·G substrate (40 nM) containing a single AP site at position 21 was treated with uracil DNA glycosylase to create an AP site, and then the AP endonuclease assay was carried out in a reaction volume of 10 μL at 37 °C for 20 min with the following concentrations of purified proteins: lanes 1 and 2, 3 and 6 ng of Gst-Apn1, respectively; lanes 3 and 4, 10 and 20 ng of Gst-Apn1(E158G), respectively; and lanes 5 and 6, 10 and 20 ng of Gst-Apn1(D192G), respectively. Purified endo IV (9 ng) was used as a positive control. Formation of the 20-mer AP endonuclease incision product was monitored by autoradiography following resolution on a 10% polyacrylamide (19:1 acrylamide:bisacrylamide ratio)−7 M urea sequencing gel. Arrows indicate positions of the 42-mer substrate and the 20-mer product. (B) Analysis of the 3′-diesterase activity. The labeled 42-mer double-stranded oligonucleotide AP site substrate was pretreated with excess purified endonuclease III to create the 20-mer product bearing the 3′-α,β-unsaturated aldehyde. Processing of this blocked end with 3′-diesterase activity creates a faster migrating 3′-hydroxyl group. The 3′-diesterase activity was performed in a reaction volume of 10 μL at 37 °C for 20 min with the same protein concentrations given for panel A. Purified endo IV (4 ng) was used as a control to cleave the AP site substrate and to reveal the position of the 3′-hydroxyl group. Arrows on the right indicate positions of the 3′-α,β-unsaturated aldehyde and 3′-hydroxyl group. (C) Analysis of the incision activity on substrates containing oxidized bases. The 5′-^{32}P-labeled duplex oligonucleotide substrates containing dHU/G (20 nM, lanes 1−5), dHT/A (20 mM, lanes 6−10), or THF/G (10 nM, lanes 11−15) were incubated with Apn1 (lanes 2, 7, and 12), Gst-Apn1 (lanes 3, 8, and 13), E158G (lanes 4, 9, and 14), and D192G (lanes 5, 10, and 15) under the same reaction conditions given for panel A. Control lanes 1 and 6 contained substrates that were treated with light piperidine. Arrows indicate the positions of the 30-mer substrates and the 10-mer product. The data are representative of two independent analyses.

with glycine abolishes the 3′-diesterase activity of this enzyme.

In addition to AP endonuclease and 3′-diesterase activities, Apn1 also possesses the ability to incise DNA at the site of oxidatively damaged bases, e.g., 5,6-dihydropyrimidines, that are the major products generated by γ-irradiation under anoxic conditions (*10*). We therefore determined if this novel enzymatic activity of Apn1 was also altered by glycine substitution at either E158 or D192. We used two independent substrates bearing either dihydrouracil paired with G

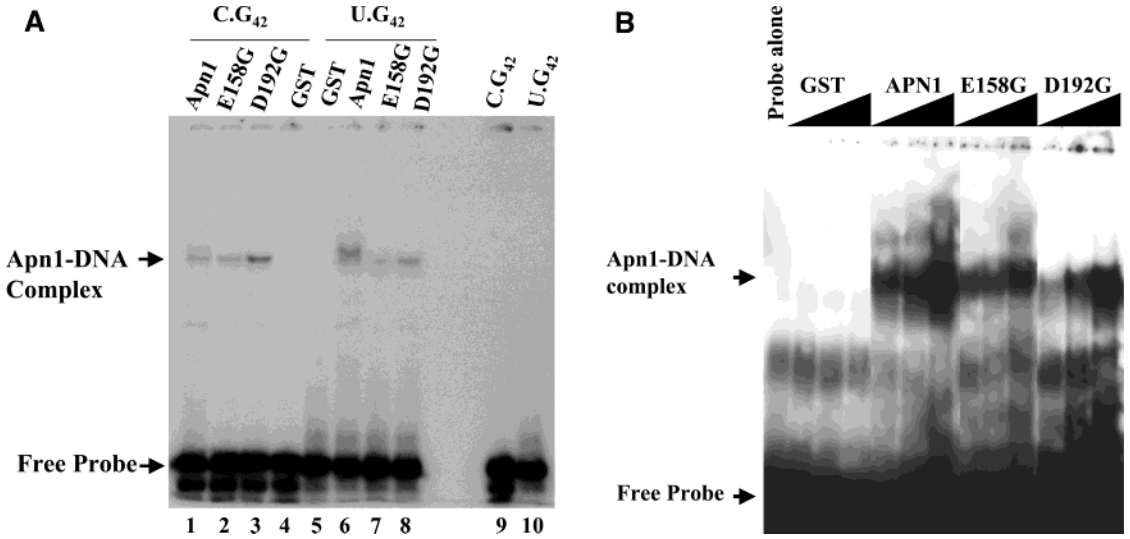

FIGURE 7: Mobility shift analysis of a natural and a mismatch-containing 42-mer-labeled double-stranded oligonucleotide by purified Gst-Apn1, Gst-Apn1(E158G), Gst-Apn1(D192G), and Gst. (A) Binding of a fixed amount of purified proteins to the 42-mer labeled oligonucleotides. The purified proteins (5 ng) were incubated with 0.1 ng of 5′-^{32}P-labeled 42-mer double-stranded oligonucleotide (1.5×10^4 cpm), either the normal (C·G, lanes 1−4) or the mismatched form (U·G, lanes 5−8), in 10 μL of buffer B for 20 min at room temperature (see Materials and Methods). The protein−DNA complexes were resolved on a 6% native polyacrylamide (19:1 acrylamide:bisacrylamide ratio) gel by electrophoresis in a high-ionic strength Tris-glycine buffer, and the protein−DNA complexes were revealed by autoradiography. (B) Binding of increasing amounts of purified proteins to the 42-mer labeled (U·G) oligonucleotide: lane 1, free probe and no protein; lanes 2−4, 10, 20, and 40 ng of purified Gst, respectively; lanes 5−7, 10, 20, and 40 ng of purified Gst-Apn1, respectively; lanes 8−10, 10, 20, and 30 ng of purified Gst-Apn1(E158G), respectively; and lanes 11−13, 5, 10, and 40 ng of purified Gst-Apn1(D192G), respectively.

(dHU/G) or dihydrothymidine paired with A (dHT/A). A third substrate bearing a modified AP site tetrahydrofuran (THF/G) was used as a control for AP endonuclease activity. Cleavage of these substrates can be monitored by the appearance of a 10-mer product on 20% denaturing polyacrylamide gels. Figure 6C revealed that the Gst-Apn1 mutants were unable to cleave the 5′-^{32}P-labeled dHU/G (lanes 4 and 5), dHT/A (lanes 9 and 10), and TFH/G substrates (lanes 14 and 15). In control experiments, cleavage of the DNA substrates with the purified Gst-Apn1 was as proficient as the untagged native Apn1 (Figure 6C, lane 3 vs lane 2, lane 8 vs lane 7, and lane 13 vs lane 12). It is noteworthy that the 5,6-dihydropyrimidines, having lost their aromatic structure, are more susceptible to base loss. As shown in Figure 6C when the dHU/G- and dHT/A-containing oligonucleotides in the absence of enzyme are treated with piperidine, they are only minimally incised (<3%), suggesting that the AP site yield is negligible. Similar results were obtained when using 3′-[^{32}P]dCMP-labeled dHU/G, dHT/A, and TFH/G substrates (data not shown). On the basis of the findings described above, we conclude that glycine substitution at either E158 or D192 of Apn1 produces variant proteins with severe defects in their ability to process DNA lesions.

Gst-Apn1 Mutants Bind to Double-Stranded Oligonucleotide. We next examined if the DNA repair defects of the Apn1 mutants could be a consequence of an inability to bind DNA. We thus monitored the binding of the purified proteins to two different double-stranded 42-mer oligonucleotides using an electrophoretic mobility shift assay (EMSA). One of the 42-mer double-stranded oligonucleotides contained a natural DNA sequence, and the other carried a central U·G mispair. Like the native Gst-Apn1, the two mutants retained the ability to bind the natural 42-mer oligonucleotide (Figure 7A, lanes 2 and 3 vs lane 1), as well as the 42-mer oligonucleotide carrying the U·G mispair (Figure 7A, lanes 7 and 8 vs lane 6). In addition, binding of the native Gst-Apn1 and the two mutants to the labeled 42-mer oligonucleotide was dependent on protein concentration (Figure 7B). Moreover, no difference in the elution profile was observed between the native Gst-Apn1 and the mutants upon chromatography on a double-stranded DNA agarose column (data not shown). These data suggest that neither of the two single-amino acid changes alters the ability of the protein to bind DNA. It is noteworthy that under identical conditions of the assay, when the native Gst-Apn1 bound to the U·G mispair 42-mer DNA, but not the native 42-mer DNA, it consistently showed a slower migration complex (Figure 7, lane 6 vs lane 1). However, this slower migration pattern was not observed with either of the two mutants (Figure 7, lanes 7 and 8). This phenomenon could be related to the mechanism by which members of the Endo IV family are proposed to recognize and bend the DNA at the site of the lesion (see the Discussion).

DISCUSSION

In this study, we created two variants of the DNA repair enzyme Apn1 from the yeast *S. cerevisiae* by replacing either the glutamate or aspartate amino acid residue at position 158 or 192, respectively, with glycine. We show that the resulting mutants E158G and D192G have no apparent defects in protein stability or in the ability to enter the nucleus or to interact with DNA. However, these variant proteins were unable to restore resistance to MMS and H_2O_2 to a DNA repair deficient yeast strain, strongly suggesting that E158 or D192 is required for Apn1 to repair damaged DNA *in vivo*. In strong support of this, the purified mutant proteins were found to be either severely or completely deficient in Apn1-associated DNA repair activities, including AP endonuclease and 3′-diesterase, as well as the incision of oxidized bases (*4*, *6*, *10*). The fact that a single-amino acid change sharply diminishes all the DNA processing activities of Apn1

strongly suggests that the different enzymatic activities of this protein are governed by the same active site. It is therefore possible that amino acid residues E158 and D192 play crucial role(s) in the enzyme catalytic center. In addition, it would appear that the function of D192 is more critical than that of E158, as the D192G substitution showed no residual enzymatic activities as compared to E158G which showed an ~150-fold reduction.

Recently, the high-resolution atomic structure of *E. coli* endo IV was determined when the enzyme is bound to a 15-mer duplex DNA containing a synthetic AP site (*27*). The crystal structure provided clear insight into the enzyme catalytic mechanism and revealed that endo IV consists of eight parallel β-strands each surrounded by peripheral α-helices in forming an $\alpha_8\beta_8$ TIM barrel fold, which is suitably arranged to bind DNA (*27*). At AP sites, the enzyme acts by compressing and bending the DNA ~90° such that it causes the orphan nucleotide and the AP site to flip out of the duplex (*27*). The AP site is then sequestered within an enzyme active site pocket, where the 5′-phosphate bond is cleaved by a trinuclear zinc cluster that renders the phosphorus atom susceptible to a nucleophilic attack (*27*). The endo IV enzyme pocket has the ability to discriminate between undamaged and damaged nucleotides (*27*). The undamaged nucleotides exist in a β-configuration and are sterically excluded from the enzyme active site pocket (*27*). However, damaged nucleotides with an α-configuration, such as dihydropyrimidines, 5-hydroxypyrimidines, and formamidopyrimidines, can be accommodated by the enzyme active site pocket, providing a reasonable explanation why members of the Endo IV family can directly incise DNA containing oxidatively damaged bases (*10*, *28*). In addition, the endo IV enzyme pocket is structured to accommodate strand breaks terminated with 3′-blocking groups such as 3′-phosphate and α,β-unsaturated aldehyde (*27*). Thus, the structural and functional conservation that exists between endo IV and Apn1 strongly suggests that Apn1 is likely to use a similar enzyme active site pocket to process DNA lesions. However, this might not be the case, as our structure−function analyses revealed some key differences between endo IV and Apn1. Previously, we have established that a mutant form of endo IV, E145G, was unable to bind to DNA (*17*). Consistent with our findings, the high-resolution structure of endo IV revealed that E145 indeed lies within one of the five DNA recognition loops, which the enzyme uses to make contact with double-stranded DNA (*27*). Surprisingly, a glycine substitution of the identical amino acid residue E158 in Apn1 did not prevent this mutant from binding to double-stranded DNA, suggesting that E158 may play a single role, perhaps making contact only with the metal ions required for catalysis, while the endo IV E145 residue plays a dual role in DNA binding and coordinating the trinuclear Zn cluster (*17*, *27*).

Another key difference between Apn1 and endo IV lies within one of the most conserved stretches of amino acid residues (^{175}GVCI**D**TCH^{182}) shared by the Endo IV family. In this region, replacement of the aspartate with glycine (D179G) reduces endo IV enzymatic activities by nearly 40-fold (*17*). According to the endo IV crystal structure, Asp179 plays a role by stabilizing the positions of two of the three Zn (Zn2 and Zn3) atoms within the trinuclear Zn cluster required for the enzyme catalytic reaction (*27*). In the case of Apn1, we found that the corresponding Asp192 residue showed no residual enzymatic activities. It is unlikely that differences in the Zn atom content can account for the disparity in the enzyme level of the endo IV and Apn1 mutants, as atomic absorption spectrometry revealed that Apn1 also contains at least three Zn atoms (*29*). A reasonable explanation would be provided if one of the Zn atoms of Apn1 is only weakly held in the active site pocket by Asp192, as compared to endo IV where the Zn atoms are held in place by the side chains of multiple amino acid residues. In fact, Apn1 treated with the metal chelator 1,10-phenanthroline can be reactivated by addition of $ZnCl_2$, but not endo IV treated in a similar manner (*29*). If indeed Asp192 forms a metal ligand, it is likely that the D192G mutant could have a lower Zn content, although addition of $ZnCl_2$ did not reactivate either the E158G or D192G Apn1 mutant (data not shown). We anticipate that crystallographic studies of this D192G mutant of Apn1 in the presence of duplex DNA bearing an AP site should clearly define the role of this important amino acid residue.

We believe that the native Gst-Apn1 purified from *E. coli* may possess an intrinsic 3′- to 5′-exonuclease activity, which removes additional nucleotides following cleavage of the AP site. In fact, a recent study also documented that Gst-Apn1 purified from yeast can remove additional nucleotide(s) in the 3′- to 5′-direction at a nick in double-stranded DNA to create a gap, although removal of the first nucleotide appears to be more rapid (*25*). If indeed the 3′- to 5′-exonuclease activity is an inherent property of Apn1, as recently demonstrated for endo IV (*30*), then this activity could be regulated perhaps through protein−protein interaction as observed for Apn2 (*31*), and play an important function in maintaining the fidelity of DNA polymerase by removing incorrectly incorporated bases.

ACKNOWLEDGMENT

We are indebted to Dr. Elliot Drobetsky, Dr. Thomas Wilson, and Andrea Shatilla for critically reading the manuscript.

REFERENCES

1. Demple, B., and Harrison, L. (1994) *Annu. Rev. Biochem. 63*, 915−948.
2. Ramotar, D. (1997) *Biochem. Cell Biol. 75*, 327−336.
3. Ramotar, D., Kim, C., Lillis, R., and Demple, B. (1993) *J. Biol. Chem. 268*, 20533−20539.
4. Ramotar, D., Popoff, S. C., Gralla, E. B., and Demple, B. (1991) *Mol. Cell. Biol. 11*, 4537−4544.
5. Vongsamphanh, R., Fortier, P. K., and Ramotar, D. (2001) *Mol. Cell. Biol. 21*, 1647−1655.
6. Johnson, A. W., and Demple, B. (1988) *J. Biol. Chem. 263*, 18017−18022.
7. Singhal, R. K., Prasad, R., and Wilson, S. H. (1995) *J. Biol. Chem. 270*, 949−957.
8. Matsumoto, Y., and Kim, K. (1995) *Science 269*, 699−702.
9. Johnson, A. W., and Demple, B. (1988) *J. Biol. Chem. 263*, 18009−18016.
10. Ischenko, A. A., and Saparbaev, M. K. (2002) *Nature 415*, 183−187.
11. Gibbs, P. E., and Lawrence, C. W. (1995) *J. Mol. Biol. 251*, 229−236.
12. Kunz, B. A., Henson, E. S., Roche, H., Ramotar, D., Nunoshiba, T., and Demple, B. (1994) *Proc. Natl. Acad. Sci. U.S.A. 91*, 8165−8169.

13. Masson, J. Y., and Ramotar, D. (1997) *Mol. Microbiol. 24*, 711−721.
14. Bennett, R. A. (1999) *Mol. Cell. Biol. 19*, 1800−1809.
15. Johnson, R. E., Torres-Ramos, C. A., Izumi, T., Mitra, S., Prakash, S., and Prakash, L. (1998) *Genes Dev. 12*, 3137−3143.
16. Ramotar, D., and Demple, B. (1996) *J. Biol. Chem. 271*, 7368−7374.
17. Yang, X., Tellier, P., Masson, J. Y., Vu, T., and Ramotar, D. (1999) *Biochemistry 38*, 3615−3623.
18. Sherman, F., Fink, G., and Hicks, J., Eds. (1983) *Methods in yeast genetics*, Cold Spring Harbor Laboratory Press, Plainview, NY.
19. Jilani, A., Ramotar, D., Slack, C., Ong, C., Yang, X. M., Scherer, S. W., and Lasko, D. D. (1999) *J. Biol. Chem. 274*, 24176−24186.
20. Bradford, M. M. (1976) *Anal. Biochem. 72*, 248−254.
21. Shatilla, A., and Ramotar, D. (2002) *Biochem. J. 365*, 547−553.
22. Jurado, J., Saparbaev, M., Matray, T. J., Greenberg, M. M., and Laval, J. (1998) *Biochemistry 37*, 7757−7763.
23. Saparbaev, M., and Laval, J. (1994) *Proc. Natl. Acad. Sci. U.S.A. 91*, 5873−5877.
24. Audet, J. F., Masson, J. Y., Rosen, G. D., Salesse, C., and Guerin, S. L. (1994) *DNA Cell Biol. 13*, 1071−1085.
25. Vance, J. R., and Wilson, T. E. (2001) *Mol. Cell. Biol. 21*, 7191−7198.
26. Ramotar, D., Popoff, S. C., and Demple, B. (1991) *Mol. Microbiol. 5*, 149−155.
27. Hosfield, D. J., Guan, Y., Haas, B. J., Cunningham, R. P., and Tainer, J. A. (1999) *Cell 98*, 397−408.
28. Ide, H., Tedzuka, K., Shimzu, H., Kimura, Y., Purmal, A. A., Wallace, S. S., and Kow, Y. W. (1994) *Biochemistry 33*, 7842−7847.
29. Levin, J. D., Shapiro, R., and Demple, B. (1991) *J. Biol. Chem. 266*, 22893−22898.
30. Kerins, S. M., Collins, R., and McCarthy, T. V. (2002) *J. Biol. Chem. 278*, 3048−3054.
31. Unk, I., Haracska, L., Gomes, X. V., Burgers, P. M., Prakash, L., and Prakash, S. (2002) *Mol. Cell. Biol. 22*, 6480−6486.

BI034163M